Available online at www.sciencedirect.com
SCIENCE DIRECT®
ELSEVIER
Journal of Magnetism and Magnetic Materials 290–291 (2005) 1398–1401
Journal of magnetism and magnetic materials
www.elsevier.com/locate/jmmm

Clustering of Mn in (Ga,Mn)As

H. Raebiger[a,*], A. Ayuela[b], J. von Boehm[a], R.M. Nieminen[a]

[a]*COMP/Laboratory of Physics, Helsinki University of Technology, POB 1100, 02015 HUT, Finland*
[b]*Donostia International Physics Centre (DIPC), POB 1072, 20018 Donostia, Spain*

Available online 15 December 2004

Abstract

Clustering of (Ga,Mn)As is studied with the supercell density-functional calculations using the projector augmented-wave method. We find large binding energies for a single substitutional Mn atom to existing dimers and trimers giving rise to trimer and tetramer formation. For larger clusters this binding energy drops. In all cases studied, ferromagnetic alignment is found to be energetically more favourable than the antiferromagnetic one.

PACS: 75.50.Pp; 85.75.−d

Keywords: Clusterization; Diluted magnetic semiconductors

1. Introduction

Inclusion of Mn into the GaAs semiconductor leads to a diluted magnetic semiconductor with a relatively high Curie temperature ($T_C \sim 100$ K) [1–3]. The ferromagnetic coupling between the Mn atoms is generally believed to be mediated by the holes that are created by the Mn atoms when they substitute Ga atoms. In principle, each substitutional Mn atom (Mn_{Ga}) should create one hole. However, in reality only a fraction of the expected number of holes is found in epitaxially grown samples (0.03–0.3 of the Mn concentration) [3,4]. The As antisites (As_{Ga}) and Mn interstitials (Mn_i), both acting as donors, are proposed to be responsible for this hole compensation [5–13]. Post-growth annealing close to the epitaxial growth temperature can enhance considerably the hole concentration and conductivity as well as T_C [5,6,10,14]. However, a prolonged annealing reduces these quantities again [5,6]. This behaviour implies that at least two processes are operating simultaneously. Several possible processes were suggested including various clustering mechanisms [5,6,10,15]. Recently, Edmonds et al. [16] showed that post-growth annealing close to the epitaxial growth temperature removes Mn_i and enhances T_C up to 159 K. Still this is considerably less than theoretical predictions [17], which suggests the presence of other mechanisms.

Even in the ideal case of random Mn substitution onto the Ga sublattice small amounts of clusters exist. Structural evolution during epitaxial growth and post-growth annealing can lead to further clustering. Sullivan et al. [18] found Mn_{Ga}–Mn_{Ga} pairs and complexes of Mn_{Ga} and Mn_i in as-grown samples from cross-sectional scanning tunneling microscopy images analysed with first-principles calculations. Mn clustering/clusters have been studied theoretically using first-principles methods. Schilfgaarde and Mryasov used linear muffin-tin orbital atomic spheres approximation (LMTO-ASA) within the local spin-density (LSD) approximation to calculate exchange integrals for Heisenberg Hamiltonian

*Corresponding author. Tel.: +358 9 451 3108; fax: +358 9 451 3116.
E-mail address: hra@fyslab.hut.fi (H. Raebiger).

0304-8853/$ - see front matter © 2004 Elsevier B.V. All rights reserved.
doi:10.1016/j.jmmm.2004.11.447

and concluded that magnetic exchange interactions deviate strongly from simple model considerations [19]. Mahadevan and Zunger used the plane wave ultrasoft pseudopotentials method and found among other results a highly stable Mn_{Ga}–Mn_i–Mn_{Ga} cluster [20]. Our purpose here is to study Mn_{Ga} clusters up to and including five Mn atoms with all-electron accuracy.

2. Methods

Total energies are calculated using the density-functional theory in the generalized gradient approximation (GGA-PW91) and the projector augmented-wave (PAW) method implemented in the VASP code [21]. We tested for the zinc-blende MnAs structure that the PAW method gives results which are in close agreement with the results obtained with the all-electron full-potential linearized augmented plane wave method [22]. The same experimental lattice constant $a = 5.65\,\text{Å}$ is used throughout. The Mn clusters are studied in supercells, containing 64, 96 or 128 atoms corresponding to 2×2×2, 2×2×3 and 2×2×4 cubic zinc-blende unit cells, respectively. In these supercells we include up to and including five Mn atoms at substitutional Ga sites, which corresponds to experimentally relevant Mn concentrations ($\frac{1}{16}$–$\frac{5}{64}$ or about 6.3–7.8 %). Due to the metallic band structure a dense k-point mesh must be used for Brillouin zone integrations. We use a Monkhorst Pack $(0.14\,\text{Å}^{-1})^3$ sampling mesh including the Γ point. Plane waves are included up to a 275 eV cutoff. The total energy is calculated in the cases of uniformly distributed Mn atoms and substitutional Mn clusters. In the 64 atom supercell, all atomic positions are relaxed. The changes in the electronic structure and the atomic positions are negligible; therefore only the ideal lattice positions are used in the larger supercells.

3. Results and discussion

We find that the ferromagnetic high symmetry configurations consisting of nearest neighbour Mn_{Ga}'s are energetically most favourable. These clusters (single Mn, Mn dimer, 60° trimer, tetramer, and pentamer) are shown in Fig. 1 together with other calculated trimers. The total energies for various ferromagnetic configurations are given in Table 1, and from these values we investigate the energy for one distant Mn_{Ga} to bind ferromagnetically to the most stable cluster. These binding energies are plotted in Fig. 2(a). The maximum value at (3 + 1) corresponds to tetramer formation. The energy gain in forming pentamers is smaller than the energy required to dissociate existing trimers and tetramers, i.e. larger clusters will not grow at the cost of smaller ones.

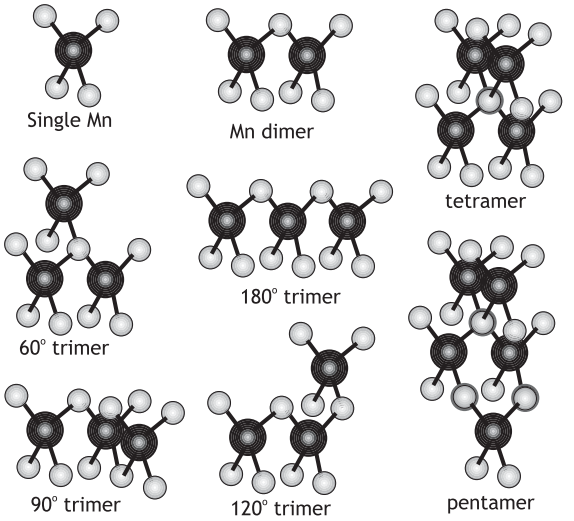

Fig. 1. Most stable calculated clusters: single Mn, Mn dimer, 60° trimer, tetramer ($x = 6.3\%$), and pentamer ($x = 7.8\%$). Also some more open trimers ($x = 6.3\%$) are shown.

Table 1
Calculated total energy differences for Mn clusters at $x = 6.3\%$ except for the pentamer at $x = 7.8\%$

Configuration	E_{FM} (meV)	Δ_{AFM-FM} (meV)	
64 *Atom supercell*, $x = 6.3\%$			
Dimer	0 ↑↑	211 ↑↓	
Single Mn + single Mn	114 ↑ · ↑	171 ↑ · ↓	
96 *Atom supercell*, $x = 6.3\%$			
60° Trimer	0 ↑↑↑	331 ↑↓↑	
90° Trimer	130 ↑↑↑	416 ↑↓↑	193 ↑↑↓
120° Trimer	198 ↑↑↑	385 ↑↓↑	208 ↑↑↓
180° Trimer	126 ↑↑↑	341 ↑↓↑	223 ↑↑↓
Dimer + single Mn	233 ↑↑ · ↑	266 ↑↓ · ↑	133 ↑↑ · ↓
128 *Atom supercell*, $x = 6.3\%$			
Tetramer	0 ↑↑↑↑		
60° Trimer + single Mn	271 ↑↑↑ · ↑		
Dimer + dimer	342 ↑↑ · ↑↑		
128 *Atom supercell*, $x = 7.8\%$			
Pentamer	0 ↑↑↑↑↑		
Tetramer + single Mn	150 ↑↑↑↑ · ↑		
60° Trimer + dimer	223 ↑↑↑ · ↑↑		

All Mn atoms are at substitutional Ga positions. The angle is the Mn–Mn–Mn angle. E_{FM} denotes the energy of a ferromagnetic cluster with respect to the ground state. Δ_{AFM-FM} gives the energy of the cluster in the spin-configuration indicated (at present only one spin is flipped) with respect to the corresponding ferromagnetic configuration.

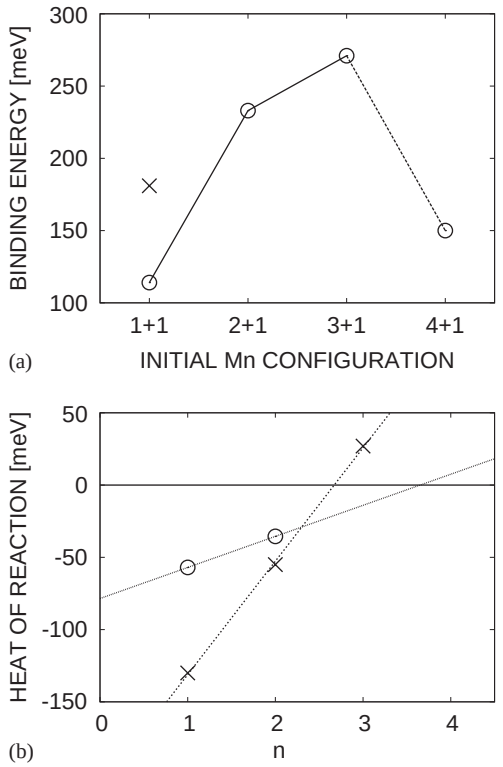

Fig. 2. (a) Calculated binding energies for one distant Mn_{Ga} to bind ferromagnetically to the most stable cluster. The three first data points are calculated for $x = 6.3\%$ and the last one for $x = 7.8\%$. (b) Calculated heat of reaction values. "o" - calculated values; "x" -from Ref. [19].

To compare our results with Ref. [19] we have calculated the heat of the reaction for decomposing a pair of n atom clusters into an $n+1$ and an $n-1$ clusters, described as

$$Mn_nGa_{N-n}As_N \rightarrow \frac{1}{2}(Mn_{n+1}Ga_{N-n-1}As_N + Mn_{n-1}Ga_{N-n+1}As_N).$$

Here n denotes the number of Mn_{Ga}'s and N the number of atoms in the sublattice of one supercell. Our values (circles in Fig. 2(b)) exhibit smaller binding for the dimer than the LSD-LMTO-ASA calculation [19] (crosses). This overbinding in Ref. [19] can partially be ascribed to the use of the LSD instead of GGA. The optimal cluster size corresponding to the crossing $E(n) = 0$ will also be different. Ref. [19] gives an optimal cluster size slightly below $n = 3$. Our binding energy maximum (Fig. 2(a)) is around $n = 4$, and linear extrapolation in Fig. 2(b) would lead to the same value.

As mentioned above, the most stable Mn_{Ga} clusters are ferromagnetically aligned (and symmetric). As expected, the intra-cluster ferromagnetic coupling is strong. For example, the spin flip energies for the middle spin of trimers range about 0.3–0.4 eV (see Table 1). Preliminary calculations show that intracluster ferromagnetic coupling has the tendency to strengthen in larger clusters (not given in Table 1). Ferromagnetic coupling is long ranged because in the separated $Mn_{Ga} + Mn_{Ga}$ case the spin flip requires an energy of 171 meV and the spin flip of an Mn_{Ga} further away from a dimer still requires an energy of 133 meV.

In conclusion, we consider here Mn complexing only on ideal Ga sites, and find this kind of clustering energetically favourable. Our study does not rule out complexing of Mn_{Ga} with e.g. Mn_i or As_{Ga} studied in Refs. [20,23], which also can be experimentally relevant.

Acknowledgements

This work has been supported by the Academy of Finland through the Center of Excellence Program (2000–2005). The authors thank Professor K. Saarinen and F. Tuomisto for many valuable discussions. We acknowledge the generous computing resources of the Center for the Scientific Computing (CSC).

References

[1] H. Ohno, A. Shen, F. Matsukura, A. Oiwa, A. Endo, S. Katsumoto, Y. Iye, Appl. Phys. Lett. 69 (1996) 363.
[2] F. Matsukara, H. Ohno, A. Shen, Y. Sugawara, Phys. Rev. B 57 (1998) R2037.
[3] H. Ohno, J. Magn. Magn. Mater. 200 (1999) 110.
[4] S. Koshihara, A. Oiwa, M. Hirasawa, S. Katsumoto, Y. Iye, C. Urano, H. Yakagi, H. Munekata, Phys. Rev. Lett. 78 (1997) 4617.
[5] T. Hayashi, Y. Hashimoto, S. Katsumoto, Y. Iye, Appl. Phys. Lett. 78 (2001) 1691.
[6] S. Potashnik, K. Ku, S. Chun, J. Berry, N. Samarth, P. Schiffer, Appl. Phys. Lett. 79 (2001) 1495.
[7] P.A. Korzhavyi, I.A. Abrikosov, E.A. Smirnova, L. Bergqvist, P. Mohn, R. Mathieu, P. Svedlindh, J. Sadowski, E.I. Isaev, Yu.Kh. Vekilov, O. Eriksson, Phys. Rev. Lett. 88 (2002) 187202.
[8] S. Sanvito, N. Hill, J. Magn. Magn. Mater. 242–245 (2002) 441.
[9] F. Maca, J. Masek, Phys. Rev. B 65 (2002) 235209.
[10] K.M. Yu, W. Walukiewicz, T. Wojtowicz, I. Kuryliszyn, X. Liu, Y. Sasaki, J.K. Furdyna, Phys. Rev. B 65 (2002) 201303.
[11] S.C. Erwin, A.G. Petukhov, Phys. Rev. Lett. 89 (2002) 227201.
[12] L. Bergqvist, P.A. Korzhavyi, B. Sanyal, S. Mirbt, I.A. Abrikosov, L. Nordstrom, E.A. Smirnova, P. Mohn, P. Svedlindh, O. Eriksson, Phys. Rev. B 67 (2003) 205201.
[13] G. Mahieu, P. Gondette, B. Grandidier, J. Nys, G. Allan, D. Stievenard, P. Ebert, H. Shimizu, M. Tanaka, Appl. Phys. Lett. 82 (2003) 712.

[14] K. Edmonds, K. Wang, R. Campion, A. Neumann, N. Farley, B. Callagher, C. Foxon, Appl. Phys. Lett. 81 (2002) 4991.
[15] F. Tuomisto, K. Pennanen, K. Saarinen, J. Sadowski, Phys. Rev. Lett. 93 (2004) 055505.
[16] K.W. Edmonds, P. Boguslawski, K.Y. Wang, R.P. Campion, S.N. Novikov, N.R.S. Farley, B.L. Gallagher, C.T. Foxon, M. Sawicki, T. Dietl, M. Buongiorno Nardelli, J. Bernholc, Phys. Rev. Lett. 92 (2004) 037201.
[17] K. Sato, P.H. Dederichs, H. Katayama-Yoshida, Europhys. Lett. 61 (2003) 403.
[18] J.M. Sullivan, G.I. Boishin, L.J. Whitman, A.T. Hanbicki, B.T. Jonker, S.C. Erwin, Phys. Rev. B 68 (2003) 235324.
[19] M. van Schilfgaarde, O.N. Mryasov, Phys. Rev. B 63 (2003) 233205.
[20] P. Mahadevan, A. Zunger, Phys. Rev. B 68 (2003) 075202.
[21] G. Kresse, J. Furthmüller, Phys Rev. B 54 (1996) 11169;
G. Kresse, J. Furthmüller, VASP the Guide, Vienna University of Technology, Vienna, 1999. [http://www.-tuwien.ac.at/~vasp/guide/vasp.html].
[22] H. Raebiger, A. Ayuela, R.M. Nieminen, J. Phys.: Condens. Matter 16 (2004) 457.
[23] S. Sanvito, N.A. Hill, Appl. Phys. Lett. 78 (2001) 3493.